Russian Chemical Reviews **76** (12) 1085 – 1092 (2007) © 2007 Russian Academy of Sciences and Turpion Ltd

DOI 10.1070/RC2007v076n12ABEH003732

Investigation of matrix-isolated species: spectroscopy and molecular modelling

A V Nemukhin, L Yu Khriachtchev, B L Grigorenko, A V Bochenkova, M Räsänen

Contents

I.	Introduction	1085
II.	Matrix effects in the spectroscopy of SH radicals in krypton matrices	1085
III.	Structure and spectra of the HArF molecule in argon matrices	1088
IV.	Structure and dynamics of HXeOH in water clusters	1089
V.	Conclusion	1090

Abstract. The results of experimental and theoretical approaches to the study of some stable and unstable chemical species in low-temperature noble gas matrices are considered. The characteristic features of matrix effects manifested in the spectra of the SH radicals in krypton matrices are discussed. The structure and the spectra of HArF in argon matrices and the structure and dynamics of the intermolecular complexes HXeOH with water are analysed. The bibliography includes 55 references.

I. Introduction

Cryochemistry is concerned with the structure and properties of substances at low temperatures.[1] Using methods of cryochemistry, it is possible to obtain and stabilise chemically unstable species and compounds; to this end, the species are isolated from one another in inert matrices (most often, in solid noble gases) at temperatures that preclude thermal diffusion. Matrix-isolated chemical species are traditionally studied using various spectroscopic methods.[2] (The term 'chemical species' usually refers to any molecular system: atoms, molecules, ions, radicals or intermolecular complexes.)

In recent years, studies dealing with matrix-isolated species have been carried out in a number of laboratories all over the world. One trend of such studies is the synthesis of chemical compounds of noble gases.[3–5] One more important trend is the study of photodissociation of small molecules in solid noble gas matrices.[6] These two trends are closely interrelated, because, on the one hand, the synthesis of inert gas compounds always includes the step of photolysis and, on the other hand, studies of compounds formed upon insertion of chemical species into a noble gas matrix provide important information concerning the dynamics of a photochemical process.[7,8]

Identification of matrix-isolated species based on their low-temperature vibrational and/or electronic spectra is a challenge. The solution of this problem requires advanced experimental equipment, reliable procedures, experienced researchers and often good fortune. Molecular modelling techniques based on quantum theory form an essential part of these studies.

This review presents several examples of experimental and theoretical studies of stable and unstable chemical species isolated in low-temperature noble gas matrices: SH radicals in krypton matrices, HArF species in argon matrices and intermolecular complexes HXeOH in water clusters. These studies have recently been carried out at the Departments of Chemistry of the M V Lomonosov Moscow State University and the University of Helsinki.

II. Matrix effects in the spectroscopy of SH radicals in krypton matrices

The interest in the photochemistry of SH radicals, close analogues of OH radicals, is due first of all to the topicality of studies of photochemical processes taking place in the atmosphere.[9] Free OH and SH radicals are investigated most often by spectroscopic methods. The spectra of the SH radical in the gas phase and in the van der Waals clusters SH · Rg (Rg is a noble gas: Ne, Ar, Kr) have been reported.[10] However, spectroscopic studies in condensed media, in particular, in low-temperature noble gas matrices, are required to obtain a more comprehensive picture of the properties of this species. Yet another reason for the interest in matrix-isolated SH radicals is related to noble gas chemistry. For example, upon annealing of a xenon matrix containing SH and H species, the formation of the HXeSH molecule was detected.[11]

The luminescence spectra of SH corresponding to the transition between the ground ($X^2\Pi$) and the first excited ($A^2\Sigma^+$) states

$$A^2\Sigma^+ \leftarrow X^2\Pi,$$

were recorded in various low-temperature matrices.[12] (In the interpretation of these spectra, differences between OH and SH radicals were taken into account.) However, the spectra

A V Nemukhin, B L Grigorenko, A V Bochenkova Department of Chemistry, M V Lomonosov Moscow State University, Leninskie Gory, 119992 Moscow, Russian Federation. Fax (7-495) 939 02 83, tel. (7-495) 939 10 96, e-mail: anem@lcc.chem.msu.ru, anemukhin@yahoo.com (A V Nemukhin), bella@lcc.chem.msu.ru, bell_grig@yahoo.com (B L Grigorenko), tel. (7-495) 939 48 40, e-mail: anastasia.bochenova@gmail.com (A V Bochenkova)
L Yu Khriachtchev, M Räsänen Department of Chemistry, University of Helsinki, A I Virtasen 1, FIN-00014 Helsinki, Finland. Fax (35-89) 191 50279, tel. (35-89) 191 50310, e-mail: leonid.hriachtchev@helsini.fi (L Yu Khriachtchev), tel. (35-89) 191 50281, e-mail: markku.rasanen@helsini.fi (M Räsänen)

Received 4 June 2007
Uspekhi Khimii **76** (12) 1163 – 1170 (2007); translated by Z P Bobkova

recorded in a krypton matrix differed from the spectra recorded in other matrices.[13] Detailed investigation of the luminescence spectra of SH in krypton led to a conclusion that the specific behaviour of the species isolated in a solid matrix is a result of a change in the electronically excited state of the species caused by the interaction with the matrix Kr atoms.[14, 15] Thus, in this case, we are dealing with the so-called 'matrix effect'.

Figure 1 shows the characteristic luminescence spectrum of SH radicals in solid krypton at 7.5 K.[13] The SH species were generated by photolysis of H_2S induced by an excimer laser ($\lambda = 193$ nm) mainly according to the reaction

$$H_2S \longrightarrow SH + H.$$

After electronic excitation of the photolysis products, the luminescence spectra were recorded on a Spec 270M spectrophotometer with a resolution of 0.3 nm. A specific feature of the spectra is the presence of two peaks, at 375 (hereinafter referred to as peak *I*) and 413 nm (peak *II*) corresponding to excited states of the molecule with different lifetimes. It was found experimentally that peaks *I* and *II* refer to the transition between the first excited $A^2\Sigma^+$ ($v' = 0$) and the ground $X^2\Pi$ (v'') electronic states of the SH radical. By processing the kinetic data, the lifetimes of the states for both peaks were estimated as 350 (peak *I*) and 750 ns (peak *II*).

On the basis of the results of spectroscopic studies, it was suggested that the presence of two peaks in the SH luminescence spectra in a krypton matrix is due to different trapping sites of this radical by the matrix.[13] Molecular modelling of the dynamics of the SH radical in solid krypton made it possible to substantiate this statement and identify the trapping sites.

The general strategy of modelling of matrix effects is as follows. A heterogeneous cluster of a specified size representing a fragment of the inert gas crystal lattice (face-centred cubic, fcc) with a cavity accommodating the SH species is used as the model. Construction of the potential energy surface (PES) of such heterocluster is a challenge. Combination of *ab initio* and semiempirical quantum chemistry methods is most reasonable. The former are used to describe the structure and dynamics of the embedded molecule, while the latter are used to calculate the interactions of the embedded molecule with the matrix atoms. On the basis of the chosen interaction potentials, characteristics of this heterocluster system are calculated, and the results of calculations serve as the basis for interpretation of experimental data.

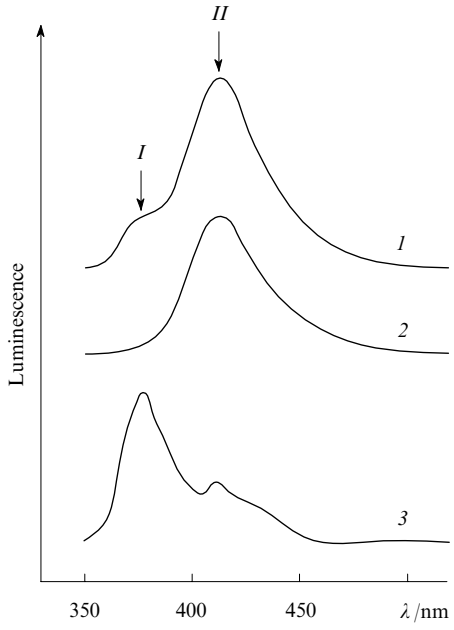


Figure 1. Experimental luminescence spectra of the SH radical in a krypton matrix at short (30 ns, curve *1*) and long (1300 ns, *2*) delay times and their difference (*3*). [Curve *3* shows the dependence of the short-lived component *I* on the wavelength; two bands can clearly be seen, which correspond to 0–0 and 0–1 transitions separated by a distance ($\sim$2500 cm^{-1}) comparable with the SH vibration frequency in the ground electronic state.]

The behaviour of the SH radical in krypton matrices has been simulated.[14] The potential energy surfaces of the heteroclusters $SH@Kr_n$ ($n \leqslant 56$) correlated with either ground [$SH(X^2\Pi) + n$ Kr] or excited [$SH(A^2\Sigma^+) + n$ Kr] states of the system were constructed by combining an *ab initio* quantum chemical method to describe the SH species and the semiempirical method using diatomic fragments in molecules (diatomics-in-molecules, DIM) for SH interaction potentials ($X^2\Pi$ or $A^2\Sigma^+$) with the Kr atoms[16] and Kr···Kr pair interaction potentials. The DIM method (see, for example, Ref. 17) is, on the one hand, an extension of the pair interaction potentials algorithm and, on the other hand, this is a semiempirical version of the valence bond theory, which allows effective inclusion of energy contributions of diatomic fragments in various electronic states to the total energy of a polyatomic molecular system.

The reliability of the potential energy surfaces of the triatomic complex SH···Kr in the ground and electronically excited states calculated by the DIM method was verified by thorough comparison of these surfaces with empirical approximations[10] of the $SH(X^2\Pi)$···Kr and $SH(A^2\Sigma^+)$···Kr surfaces derived from high-resolution spectroscopy data of the van der Waals clusters. According to these results,[10] in the ground electronic state the triatomic complex is weakly bound, the energy of its dissociation into SH in the ground state $X^2\Pi$ and a Kr atom in the ^{1}S state is about 100 cm^{-1}. The equilibrium geometry structure of the complex is linear with a distance (R_e) from the SH centre of mass to the Kr atom equal to 4.28 Å and an S–H bond length of 1.35 Å. The PES of the $SH(A^2\Sigma^+)$ + Kr(^{1}S) system in the electronically excited state has two minima separated by a saddle point. The deepest minimum with the energy of 1706 cm^{-1} corresponds to linear SH···Kr with $R_e = 3.26$ Å and $\theta = 0°$ (θ is the angle formed by the S–H bond and the straight line from the centre of mass of the SH radical to the Kr atom), while the other minimum (with the energy of $\sim$1400 cm^{-1}) corresponds to the position of the krypton atom near the SH radical on the side of the sulfur atom (Kr···SH) with $R_e = 2.6$ Å and $\theta = 180°$. The saddle point is characterised by $R_e = 4.02$ Å and $\theta = 64°$. Substantial differences in the interaction energies of the krypton atom with the SH radical occurring in the electronically excited state in different parts of the krypton matrix are responsible for the features of low-temperature spectra of SH, namely, the presence of two peaks in the luminescence spectrum (see Fig. 1). Figure 2 shows the plots for the DIM-calculated potentials of the ground (*a*) and excited (*b*) states of the triatomic complex.

It is noteworthy that representing the interaction potentials of species in the $SH@Kr_n$ clusters in terms of the DIM approximation calculated for each group of three atoms $SHKr_i$ ($i = 1, ..., n$) and the $Kr_i - Kr_j$ pair potentials allows one to estimate the energies and forces acting on atoms and use them for calculating the molecular dynamic (MD) trajectories of species.

Firsov *et al.*[15] simulated the spectrum of the SH radical in the krypton matrix corresponding to the electronic transition $A^2\Sigma^+$ ($v' = 0$) → $X^2\Pi$ (v'') using a version of mixed quantum

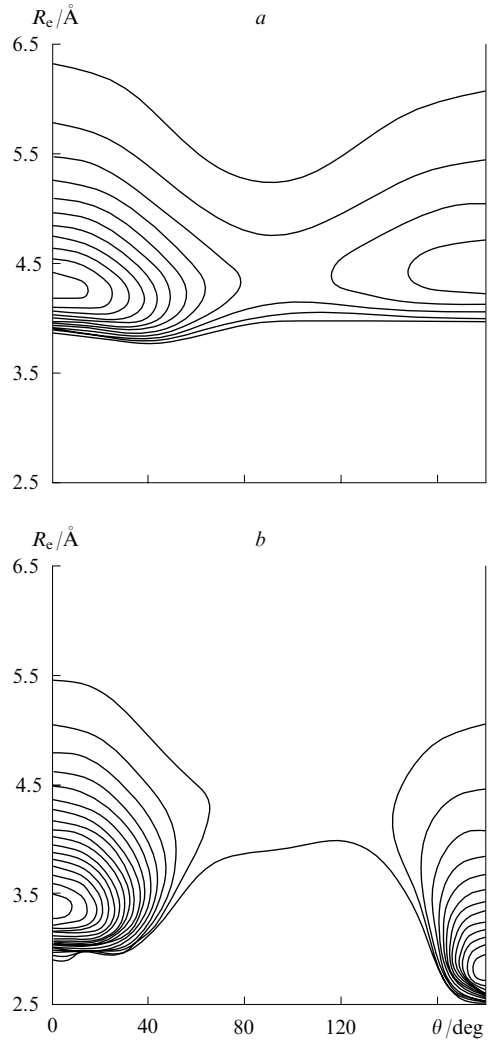


Figure 2. Potential energy surfaces of the ground (*a*) and electronically excited (*b*) states of the triatomic complex SH···Kr. The contour lines for the ground state are drawn every 10 cm^{-1}, those for the excited state are drawn every 100 cm^{-1}.

and classical molecular dynamics.† In this approximation, the SH radical with a random orientation of the S—H bond was placed on a random site in the central part of the fcc lattice composed of 256 Kr atoms (the lattice parameter was 5.67 Å). Then the Kr atoms located closely to S or H atom were removed; as the closeness criterion, distances of 2.9 Å on the side of sulfur and of 2.5 Å on the side of hydrogen were used. Then MD trajectories were calculated in two stages. In the first stage, which was 1 ps long, the system temperature was maintained at 7 K by correcting (scaling) the species velocities on the PES of the ground state of the $SH(X^2@)Kr_n$ cluster. In the second stage, the calculation was carried out for the PES of the excited state of the $SH(A^2\Sigma^+)@Kr_n$ cluster with the system energy being maintained constant. The second stage of about 10 ps long was split into 20 000 steps. Every 10 steps (2000 times over the trajectory), the electron transition wavelengths and intensities (the Franck–Condon factors), radial distribution functions and particle lifetimes (τ) were found by the numerical solution of the one-dimensional Schrödinger equation along the variable corresponding to the S—H distance, and the positions of the Kr atoms located most closely to the S and H atoms were recorded for subsequent averaging. After the calculation, the average spectrum over the trajectory, the average lifetime and the average radial distribution function were estimated and the probability map for the Kr atoms to occur in various positions near the H atom was constructed. The lifetime was estimated from the formula [19] for each discrete vibrational state of the electronically excited state:

$$\tau_{\upsilon''}^{-1} = \frac{4}{3c^2}\langle \upsilon' | \Delta U^3 D^2 | \upsilon' \rangle, \quad (1)$$

where c is the velocity of light, υ' is the wave function of the lower vibrational level of the electronically excited state, ΔU is the energy difference between the ground and electronically excited states, D is the transition dipole moment of the SH radical from the ground to excited state. For calculation of the corresponding matrix elements, it was necessary to calculate the dependence of the transition dipole moment between the electronic states on the internuclear distance in SH.

Analysis of the calculated trajectories and spectra led to the conclusion that both peaks observed in the experiments (*I* and *II*, see Fig. 1) refer to two different trapping sites of the SH radical by the krypton cluster. The peak with a lower wavelength (peak *I*) corresponds to the trajectories along which the SH radical freely moves within the krypton cluster. The peak at greater wavelength (peak *II*) refers to the trajectories characterised by the formation of the triatomic complex SH···Kr, *i.e.*, the radical is bound to one atom of the Kr lattice. The calculated lifetimes of SH excited states for both types of trajectories also correlate with experimental characteristics of the luminescence spectra (Table 1).

Table 1. Experimental and theoretical characteristics of peaks in the luminescence spectra of the SH radical in the Kr matrix.

Characteristics	Peak *I*		Peak *II*	
	experiment	calculation	experiment	calculation
Peak position /nm	375	340–350	413	390–400
Lifetime /ns	350	550–600	750	800–840
Features of MD trajectories	—	free rotation of SH in Kr	—	complex SH···Kr

A more comprehensive picture of the spatial distribution of Kr atoms around the SH radical is provided by Fig. 3. Different colour intensity shows the configuration space areas corresponding to different positions of the inert gas atom located most closely (this is determined in every integration step) to the hydrogen atom. The maps are constructed in a relative coordinate system in which the H atom is always located in the origin of coordinates and the *x*-axis is directed along the S→H bond. The results validate the assumption concerning the presence of different trapping sites of the SH molecule by the krypton matrix, which is reflected in the observed experimental spectra.

In addition to providing new information on the spectroscopy of SH radicals, Refs 14 and 15 considerably contributed to the investigations into structure and dynamics of solids doped with small molecules. These studies demonstrate the possibility of observing and interpreting the trapping sites of a molecule occurring in the electronically excited state in a low-temperature krypton matrix. Previously, such effects in cryochemistry have not been reported.

† This method was first applied to describe the spectra of the Cl_2 molecule in solid neon.[18]

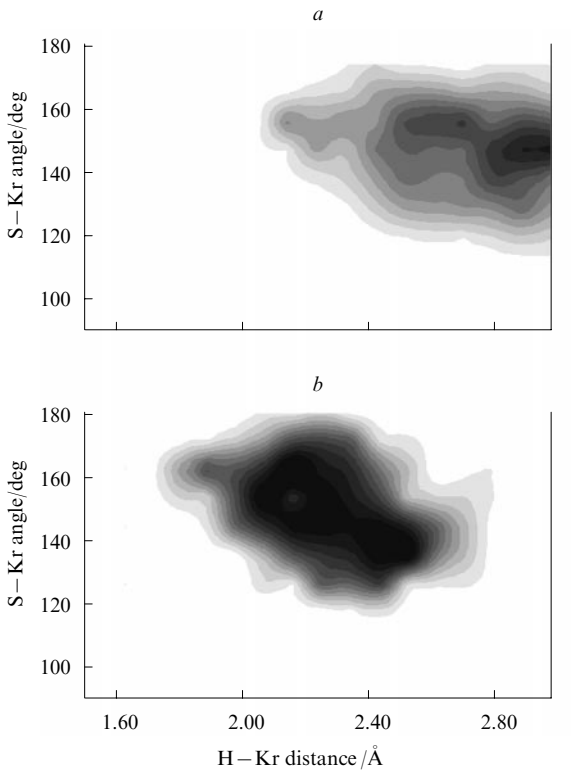


Figure 3. Distribution of the probability density for the occurrence of Kr atoms around the SH radical in the SH@Kr_n clusters;
(*a*) trajectories describing free rotation of SH in the Kr matrix (peak *I* in the luminescence spectrum of matrix isolated SH radicals);
(*b*) trajectories that tend to give SH · Kr complexes (peak *II*).

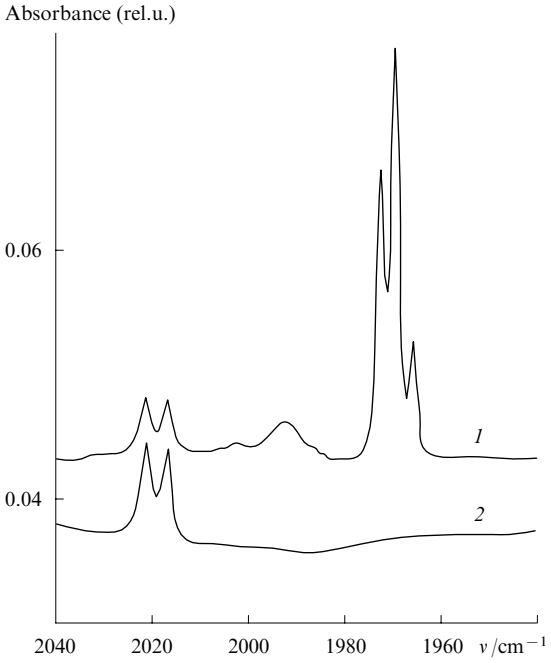


Figure 4. Spectra of the HArF molecule in solid argon recorded at matrix annealing temperatures of 20 (*1*) and 33 K (*2*). The measurements were carried out at 7 K.

III. Structure and spectra of the HArF molecule in argon matrices

As a continuation of molecular dynamics studies for interstitial compounds in low-temperature noble gas matrices, the trapping sites of the exotic HArF molecule in the ground electronic state by an argon matrix were determined. The HArF species discovered in 2000 is the first electrically neutral chemical compound of argon.[3–5] It is formed upon photodissociation of HF in solid argon at 7 K followed by matrix annealing at temperatures up to ~20 K:

$$H + Ar + F \longrightarrow HArF.$$

Initially, the formation of this compound was established by IR spectroscopy.[3–5] Subsequently, it has been shown [14] that IR spectroscopy provides knowledge also on the molecular structure and dynamics in a doped matrix.

Figure 4 shows the spectra of HArF in solid argon in the region of H—Ar stretching vibrations. Curves *1* and *2* were recorded at different matrix annealing temperatures, 20 and 33 K. The characteristic triplet of the spectral lines (1965.7, 1969.4 and 1972.3 cm^{-1}) is observed only for low annealing temperature and completely disappears at higher temperature. The doublet shifted towards larger wavenumbers (2016.3 and 2020.8 cm^{-1}) predominates, conversely, at higher annealing temperatures up to matrix destruction at 40 K. On the basis of the obtained experimental results, it was hypothesised that the triplet of the spectral lines corresponds to a thermally unstable trapping site of HArF in the argon matrix, while the doublet shifted to the blue spectral region is due to another, more stable (or thermally relaxed) trapping site of the HArF molecule in the solid argon matrix.[20–22] The use of molecular modelling confirmed this assumption and identified the trapping sites of the guest species.[23–25]

An original hybrid procedure for calculation of the PES of HArF@Ar_n heteroclusters ($n = 363$ or 364) has been reported.[23] The energy of the embedded molecule (HArF) and its first and second derivatives with respect to nuclear coordinates were calculated by the high-precision *ab initio* method MP2/6-311++G(2d,2p) using PC GAMESS software.[26] The interactions of argon atoms with one another were described by pair potentials well parametrised to many properties of this gas.[27] The interaction of HArF with each atom of the matrix was calculated in the DIM approximation taking into account contributions of ionic and neutral pair potentials. This calculation algorithm proved to be useful for modelling the properties of the HF@Ar_n clusters.[28] This combined procedure, that is, quantum mechanics with diatomics-in-molecules approximation (QM/DIM), was also successfully tested in the simulation of the spectra of gas-phase mixed $Ar_n(HCl)_m$ and $Ar_n(HF)_m$ clusters.[29]

The calculated PES for the HArF@Ar_n system was used to find the stationary points on the surface and calculate the harmonic vibration frequencies. The atom sites in the fcc lattice of the argon matrix served as the initial coordinates. Figure 5 shows two optimised structures corresponding to the trapping sites of the HArF molecule by solid argon. According to the calculation results, the structure presented in Fig. 5 *a* refers to a thermally unstable trapping site; it is responsible for characteristic spectral bands at 1970 cm^{-1} (see Fig. 4). The structure shown in Fig. 5 *b* was assigned to the stable trapping site characterised by bands at 2120 cm^{-1}.

This assignment was based on the following computation data. First, the H—Ar vibrations in the unstable structure (see Fig. 5 *a*) are responsible for a triplet of harmonic frequencies of 2203, 2204 and 2207 cm^{-1} (depending on the vacancy position in the lattice), and the harmonic frequency of 2246 cm^{-1} assigned to the stable structure (see Fig. 5 *b*) is shifted to the blue region by almost the same distance as in the experimental spectrum. Second, the energy of the unstable structure is

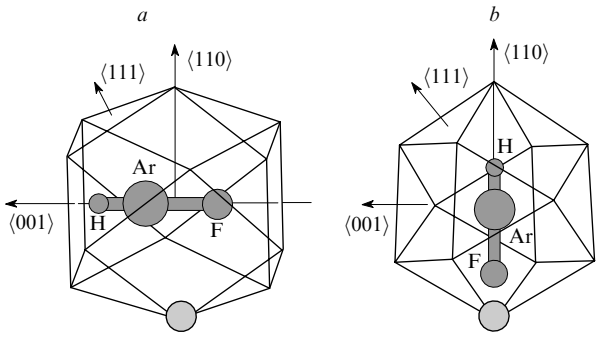


Figure 5. First solvation shells of two possible structures formed upon trapping of the HArF molecule by solid argon.
Trapping site: (*a*) unstable, (*b*) stable.

4–5 kJ mol^{-1} higher than that of the stable structure and with the possibility of matrix relaxation (*i.e.*, at higher temperature), the structure with lower energy should predominate, which was actually observed in experiments. Thus, the trapping sites of the HArF molecule by solid argon can be considered to be established. However, the thermal relaxation mechanism of the unstable configuration still remains unknown, which requires further theoretical analysis.

IV. Structure and dynamics of HXeOH in water clusters

Matrix cryochemistry methods are widely used at the University of Helsinki to study the properties of chemical compounds containing noble gas atoms.[3–5] In particular, the HXeOH species formed upon laser irradiation of a low-temperature water–xenon mixture followed by matrix annealing was detected experimentally.[30–32] The metastable species HXeOH is responsible for a local minimum in the PES of the Xe + H_2O system, whereas the complex Xe · H_2O is the major compound (having the lowest energy). It was suggested that complexes of HXeOH with water molecules may exist. This was of interest, in particular, in relation to the geochemical problem of xenon deficiency.[33,34]

Figure 6 *a,b* shows the IR spectra of a water molecule in solid xenon near the bending mode of the H_2O molecule. It can be seen that the spectra of the Xe + H_2O system with a low water content (see Fig. 6 *a*) vary with an increase in the H_2O concentration (see Fig. 6 *b*). After photolysis at 193 nm, which results in decomposition of the water molecule in the xenon matrix, and matrix annealing, which increases the mobility of the active species, the spectra exhibit the bands for HXeOH (at 1578 cm^{-1}) and two additional peaks designated in curve *3* by C_1 and C_2 (see Fig. 6 *b*). It was suggested that these peaks correspond to H–Xe vibrations in the complexes HXeOH · H_2O and HXeOH · $(H_2O)_2$, respectively. Later this hypothesis was confirmed in a theoretical study [35] dealing with molecular modelling of the intermolecular complexes of HXeOH with water. Previously, similar complexes of noble gas hydrides with nitrogen have been observed experimentally (for example, HArF · N_2 in Ref. 36) and studied by computational chemistry.[37]

The first stage of modelling included the use [35] of the combined quantum and molecular mechanics (QM/MM) method, specifically, the embedded species (HXeOH) was described by quantum chemistry methods and the surrounding water molecules were described by molecular mechanics in the effective fragment (EF) potential approximation.[38] The calculations were carried out using PC GAMESS software.[26] The computation showed that water molecules of a specified

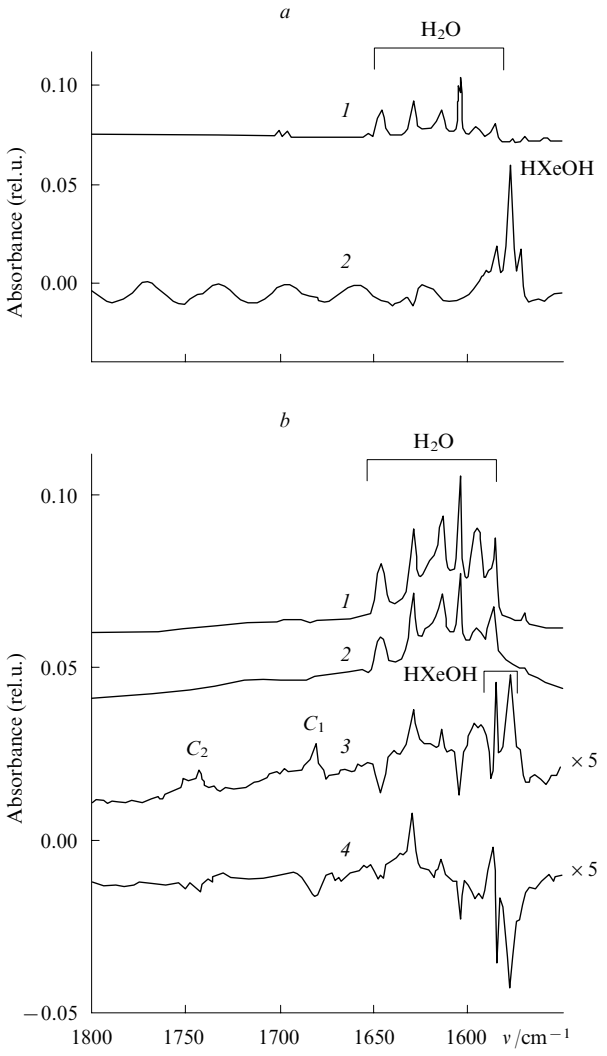


Figure 6. IR spectra of water in solid xenon recorded at low (*a*) and higher (*b*) concentrations of water;
(*a*): (*1*) spectrum recorded after condensation, (*2*) after matrix annealing;
(*b*): (*1*) spectrum recorded after condensation; (*2*) after photolysis; (*3*) after matrix annealing; (*4*) after short-term photolysis of the annealed matrix.

geometry configuration (*i.e.*, effective fragments) can form cages that completely trap HXeOH. However, these local minima in the PES proved to be artifacts of this computational procedure; on passing to a higher modelling level (by quantum chemistry techniques), the clusters containing > 3 water molecules were destroyed. In particular, the use of MP2 method with aug-cc-pVTZ basis functions on the oxygen and hydrogen atoms, Stuttgart pseudopotential [39] and the appropriate basis set (6s6p1d)/[4s4p1d] on xenon resulted in configurations of the local and global minima in the PES of the HXeOH complexes containing from one to three water molecules. Thus, it was established that the PES local minima correspond to the bound states of the HXeOH · $(H_2O)_n$ systems (n = 0–3). Figure 7 shows the calculated equilibrium structures for the complexes HXeOH · $(H_2O)_n$. These complexes may decompose through potential barriers ranging from 0.4 (for n = 3) to 39.6 kcal mol^{-1} (n = 0) to give xenon complexes with water clusters: Xe · $(H_2O)_{n+1}$, which account for the PES global minima.

Table 2 summarises the computation results for the parameters of the HXeOH · $(H_2O)_n$ complexes.

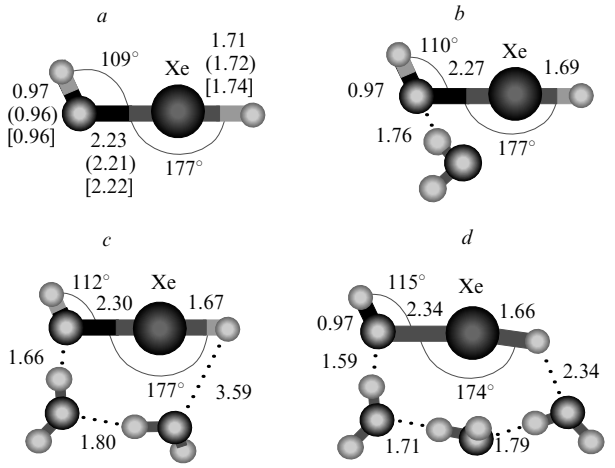


Figure 7. Equilibrium geometry configurations of the complexes $HXeOH \cdot (H_2O)_n$ for $n = 0$ (*a*), 1 (*b*), 2 (*c*), 3 (*d*) corresponding to the local minima in PES. The distances are given in Å.
[For the HXeOH molecule (*a*) the results of various *ab initio* calculations taken from Ref. 32 are given in brackets.[32]).

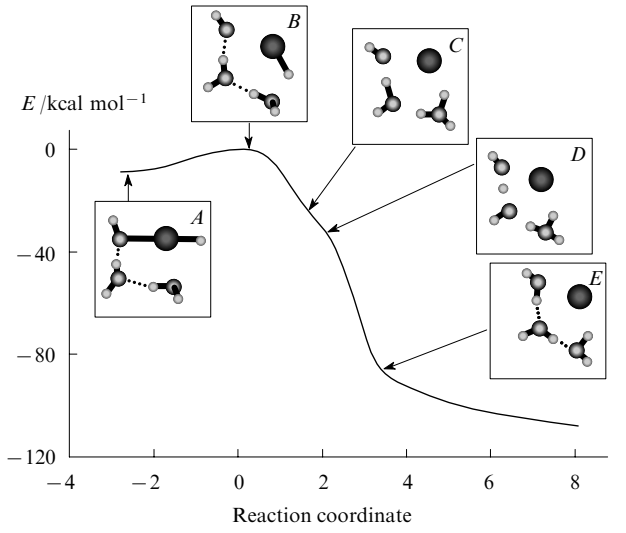


Figure 8. MP2 calculated decomposition pathway of the complex $HXeOH \cdot (H_2O)_2 \rightarrow Xe \cdot (H_2O)_3$. The insets show configurations of the metastable state of the initial complex (*A*), transition state (*B*), reaction product (*E*) and two intermediate structures along the proton transfer path (*C* and *D*).

The use of a conventional scaling procedure for the vibration frequencies calculated in the harmonic approximation permits direct comparison of the theoretically calculated frequencies and experimental positions of bands in the vibrational spectrum. If a scaling factor has been selected (*e.g.*, 0.88 based on the H—Xe stretching band in the HXeOH molecule), the theoretical estimates of the bands for the complexes $HXeOH \cdot H_2O$ and $HXeOH \cdot (H_2O)_2$ (1669 and 1735 cm^{-1}, respectively) are in good agreement with experimental data (1681 and 1742 cm^{-1}). Thus, peaks C_1 and C_2 in the spectra of matrix isolated species (see Fig. 6 *b*) are due to the HXeOH complexes with one and two water molecules. In the spectra of systems containing hydrogen bonds, the signals are shifted to the blue (short-wavelength) region with respect to the initial spectrum. Currently, such systems are under vigorous research.[40] In the case of HXeOH, the blue shift of the H—Xe frequency is attributable to additional charge transfer between the HXe and OH fragments induced by complexation with a water molecule.

Interesting results were obtained in the modelling of decomposition pathways of the $HXeOH \cdot (H_2O)_n$ complexes, *i.e.*, upon system transition from local to global minima along the reaction coordinate. To this end, configurations of the transition states as saddle points with the only vibration frequency were found. On both sides from these points, minimum energy paths to the reactant and product valleys were constructed. Figure 8 shows the calculated energy profile corresponding to decomposition of the $HXeOH \cdot (H_2O)_2$ complex. The local minimum in the beginning of the reaction path corresponds to the metastable state of the $HXeOH \cdot (H_2O)_2$ complex (*A*), transition state *B* is shown on the top of the barrier and the decomposition product $Xe \cdot (H_2O)_3$ (*E*) occurs at the end of the path. Intermediate structures *C* and *D* illustrate the proton migration along the hydrogen bond system. As the system moves from left to right, immediately after transition state *B* has been reached, the proton from the XeH^+ fragment migrates to the nearest water molecule (structure *C*). The proton from the resulting H_3O^+ species migrates to the next water molecule from which one more proton moves to the hydroxyl ion OH^- (structure *D*).

This mechanism of proton transfer along the oriented chains of water molecules illustrates the molecular scheme usually referred to as water (or proton) conductor.

Table 2. Calculated parameters of the $HXeOH \cdot (H_2O)_n$ complexes.

Parameter	$n = 0$	$n = 1$	$n = 2$	$n = 3$
Harmonic frequencies of Xe—H vibrations /cm^{-1} (relative intensities of the IR bands)	1790 (1.00)	1897 (0.77)	1972 (0.58)	2066 (0.15)
Energies of complexes (kcal mol^{-1}) with respect to the Xe + $(n+1)$ H_2O system	109.5	98.7	87.7	76.4

V. Conclusion

Despite the obvious priority of experimental works in modern chemistry and physics, the contribution of computer molecular modelling of the physicochemical properties of compounds has become rather weighty in recent years. This is due to fast progress in the computer technology, development of new effective theoretical approaches to this problem and the accumulated experience in the study of particular systems. The examples of solution of complicated problems dealing with structure determination of unstable chemical species, HArF and HXeOH, isolated in low-temperature inert gas matrices demonstrate the advantages of combined effort of experimentalists and theorists. We focused on the theoretical aspect of the studies dealing with the structures, spectra and transformation dynamics of noble gas compounds, because the experimental studies of these compounds have been the subject of recent comprehensive reviews.[4, 5]

The examples we considered are fairly typical, although they represent only a minor portion of the studies of matrix-isolated species by combinations of spectroscopic and molecular modelling methods. Consider briefly other achievements in this field of chemistry. Thus Frenking and co-workers [41, 42] predicted the structure of the stable neutral noble gas compound HeBeO using quantum chemical calculations before the experimental proof for the existence of HArF molecule was

obtained.[3] Significant for further development of this field of science are also studies by Feldman *et al.*[43–46] and Misochko *et al.*,[47–49] who analysed active species in noble gas matrices using both experimental and theoretical approaches. Chaban and co-workers [50–52] performed a number of important theoretical investigations of noble gas compounds, and the review by Gerber [53] presents a detailed discussion of the works on the structure and dynamics of these compounds. The review by McDowell [37] covers both published and author's results of quantum chemical calculations of molecules containing noble gas atoms. Finally, special mention should be made of two theoretical works [54, 55] predicting the possibility of existence of biomolecules with an inserted xenon atom on the basis of quantum chemical calculations.

Low-temperature matrix isolation has been developed as an experimental technique that allowed investigation of the properties of stable and unstable molecules isolated as fully as possible from the influence of other species. However, the progress in the instrumental equipment enabled detection of the interaction of matrix isolated compounds with the matrix material. The obtained experimental data are of interest for the development of the theory of intermolecular interactions; however, interpretation of the experimental results requires much effort.

Modern *ab initio* quantum chemistry methods provide virtually exact description of the structures and spectra of small (comprising up to 10 atoms) molecules in vacuum, *i.e.*, under conditions where they are separated from other species. Accurate calculations for intermolecular complexes, especially weakly bound complexes with noble gas atoms, are very difficult. The studies discussed in this review used the approach in which the theoretical problem was split into two levels: a matrix-isolated species was modelled by *ab initio* quantum chemistry methods, while its interaction with the matrix species was described by well parametrised semiempirical potentials, in particular, by diatomics-in-molecules potentials. Direct comparison of the calculation results obtained by this combined approach with experimental results often demonstrates the success of this strategy.

Apparently, the future development of the modelling techniques for matrix-isolated species would be related to more active use of molecular dynamics combined with *ab initio* quantum chemical calculations. This would allow direct calculation of the temperature dependences of spectra of matrix isolated species.

The authors are grateful to co-authors of their publications A A Granovskii, D A Firsov, M Pettersson, E Isoniemi, H Tanskanen and A Lignell for fruitful discussion during the research and to Professor G B Sergeev for steady interest and attention to our work. This review was written with partial financial support of the Federal Target Science and Technology Programme of the RF (Project No. 2006-RI-112.0/001/052) and of the Academy of Sciences of Finland (Project CoE CMS).

References

1. G B Sergeev, V A Batyuk *Kriokhimiya* (Cryochemistry) (Moscow: Khimiya, 1978)
2. *Chemistry and Physics of Matrix-Isolated Species* (Eds L Andrews, M Moskovits) (Amsterdam: North Holland, 1989)
3. L Khriachtchev, M Pettersson, N Runeberg, J Lundell, M Räsänen *Nature (London)* **406** 874 (2000)
4. J Lundell, L Khriachtchev, M Pettersson, M Räsänen *Low Temp. Phys.* **26** 680 (2000)
5. M Pettersson, L Khriachtchev, J Lundell, M Räsänen *Inorganic Chemistry in Focus II* (Eds G Meyer, D Naumann, L Wesemann) (Weinheim: Wiley-VCH, 2005) p. 15
6. V A Apkarian, N Schwentner *Chem. Rev.* **99** 1481 (1999)
7. L Khriachtchev, M Pettersson, M Räsänen *Chem. Phys. Lett.* **288** 727 (1998)
8. L Khriachtchev, M Pettersson, J Lundell, M Räsänen *J. Chem. Phys.* **114** 7727 (2001)
9. R P Wayne *Chemistry of Atmospheres* (2nd Ed.) (Oxford: Clarendon Press, 1991)
10. P P Korambath, X T Wu, E F Hayes, C C Carter, T A Miller *J. Chem. Phys.* **107** 3460 (1997)
11. M Pettersson, J Lundell, L Khriachtchev, E Isoniemi, M Räsänen *J. Am. Chem. Soc.* **120** 7979 (1998)
12. J Zoval, D Imre, P Ashjian, V A Apkarian *Chem. Phys. Lett.* **197** 549 (1992)
13. L Khriachtchev, M Pettersson, E Isoniemi, M Räsänen *J. Chem. Phys.* **108** 5747 (1998)
14. B L Grigorenko, L Khriachtchev, A V Nemukhin, M Pettersson, E Isoniemi, M Räsänen *J. Chem. Phys.* **110** 5836 (1999)
15. D A Firsov, B L Grigorenko, A V Nemukhin, L Y Khriachtchev, M Räsänen *Chem. Phys. Lett.* **338** 317 (2001)
16. A V Nemukhin, B L Grigorenko, A A Granovsky *Chem. Phys. Lett.* **301** 287 (1999)
17. B L Grigorenko, A V Nemukhin, V A Apkarian *J. Chem. Phys.* **108** 4413 (1998)
18. B L Grigorenko, A V Nemukhin, N V Ozhegova *Chem. Phys. Lett.* **296** 84 (1998)
19. V I Pupyshev *Opt. Spektrosk.* **63** 570 (1987) [a]
20. L Khriachtchev, M Pettersson, A Lignell, M Räsänen *J. Am. Chem. Soc.* **123** 8610 (2001)
21. L Khriachtchev, A Lignell, M Räsänen *J. Chem. Phys.* **120** 3353 (2004)
22. L Khriachtchev, A Lignell, M Räsänen *J. Chem. Phys.* **123** 64507 (2005)
23. A V Bochenkova, D A Firsov, A V Nemukhin *Chem. Phys. Lett.* **405** 165 (2005)
24. Z Bihary, G M Chaban, R B Gerber *J. Chem. Phys.* **116** 5521 (2002)
25. S Jolkkonen, M Pettersson, J Lundell *J. Chem. Phys.* **119** 7356 (2003)
26. A V Nemukhin, B L Grigorenko, A A Granovsky *Vest. Mosk. Univ., Ser. 2, Khim.* **45** 75 (2004) [b]
27. R A Aziz, H H Chen *J. Chem. Phys.* **67** 5719 (1977)
28. B L Grigorenko, A V Nemukhin, V A Apkarian *J. Chem. Phys.* **104** 5510 (1996)
29. A V Bochenkova, M A Suhm, A A Granovsky, A V Nemukhin *J. Chem. Phys.* **120** 3732 (2004)
30. L Khriachtchev, H Tanskanen, M Pettersson, M Räsänen, J Ahokas, H Kunttu, V Feldman *J. Chem. Phys.* **116** 5649 (2002)
31. L Khriachtchev, J Lundell, M Pettersson, H Tanskanen, M Räsänen *J. Chem. Phys.* **116** 4758 (2002)
32. M Pettersson, L Khriachtchev, J Lundell, M Räsänen *J. Am. Chem. Soc.* **121** 11904 (1999)
33. W A Caldwell, J H Nguyen, B G Pfrommer, F Mauri, S G Louie, R Jeanloz *Science* **277** 930 (1997)
34. C Sanloup, B C Schmidt, E M C Perez, A Jambon, E Gregoryanz, M Mezouar *Science* **310** 1174 (2005)
35. A V Nemukhin, B L Grigorenko, L Khriachtchev, H Tanskanen, M Pettersson, M Räsänen *J. Am. Chem. Soc.* **124** 10706 (2002)
36. A Lignell, L Khriachtchev, M Pettersson, M Räsänen *J. Chem. Phys.* **118** 11120 (2003)
37. S A C McDowell *Cur. Org. Chem.* **10** 791 (2006)
38. J Joseph, E D Jemmis *J. Am. Chem. Soc.* **129** 4620 (2007)
39. M S Gordon, M A Freitag, P Bandyopadhyay, J H Jensen, V Kairys, W Stevens *J. Phys. Chem. A* **105** 293(2001)
40. A Nicklass, M Dolg, H Stoll, H Preuss *J. Chem. Phys.* **102** 8942 (1995)
41. G Frenking, D Cremer *Struct. Bonding* **73** 17 (1990)
42. M Lein, J Frunzke, G Frenking *Struct. Bonding* **106** 181 (2004)
43. V I Feldman, F F Sukhov *Chem. Phys. Lett.* **255** 425 (1996)
44. V I Feldman, F F Sukhov, A Y Orlov *Chem. Phys. Lett.* **280** 507 (1997)

45. V I Feldman, F F Sukhov, A Y Orlov, I V Tyulpina *J. Am. Chem. Soc.* **125** 4698 (2003)
46. V I Fel'dman, F F Sukhov, A Yu Orlov, I V Tyul'pina, E A Logacheva, D A Tyurin *Izv. Akad. Nauk, Ser. Khim.* 1415 (2005) [c]
47. E Y Misochko, I U Goldschleger, A V Akimov, C A Wight *J. Am. Chem. Soc.* **123** 5156 (2001)
48. A V Akimov, I U Goldschleger, E Y Misochko, C A Wight *J. Phys. Chem. A* **106** 9756 (2002)
49. E Y Misochko, A V Akimov, I U Goldschleger, D A Tyurin, D N Laikov *J. Chem. Phys.* **122** 034503 (2005)
50. G M Chaban, J Lundell, R B Gerber *J. Chem. Phys.* **115** 7341 (2001)
51. Z Bihary, G M Chaban, R B Gerber *J. Chem. Phys.* **119** 11278 (2003)
52. G M Chaban *Chem. Phys. Lett.* **395** 182 (2004)
53. R B Gerber *Annu. Rev. Phys. Chem.* **55** 55 (2004)
54. J Lundell, M Pettersson, M Räsänen *Comput. Chem.* **24** 325 (2000)
55. G M Chaban *Chem. Phys. Lett.* **401** 318 (2005)

[a] — *Opt. Spectrosc. (Engl. Transl.)*
[b] — *Moscow Univ. Chem. Bull. (Engl. Transl.)*
[c] — *Russ. Chem. Bull, Int. Ed. (Engl. Transl.)*